Structure and Energetics of Isomers of the Interstellar Molecule C_5H

T. Daniel Crawford,[†,‡] John F. Stanton,*[,†] Jamal C. Saeh,[†] and Henry F. Schaefer, III[‡]

Contribution from the Institute for Theoretical Chemistry, Departments of Chemistry and Biochemistry, The University of Texas, Austin, Texas 78712-1167, and Center for Computational Quantum Chemistry, Department of Chemistry, The University of Georgia, Athens, Georgia 30602-2525

Received July 16, 1998. Revised Manuscript Received September 30, 1998

Abstract: High-level ab initio methods based on the coupled cluster approximation have been used to study properties of several isomers of the C_5H radical, a molecule of significant interest in radioastronomy. The three lowest-lying isomers [the well-known linear form (**1**) as well as two ring-chain structures, HC_2C_3 (**2**) and C_2C_3H (**3**)] lie within 30 kcal/mol with isomer **2** approximately 5 kcal/mol higher than the lowest-energy isomer **1**. The computed rotational constant for the linear isomer is within 0.7% of the value determined in previous experimental analyses. Transition states formed via simple ring-opening mechanisms for the interconversion of the linear and ring-chain isomers have also been located; these lie ca. 27 and 31 kcal/mol above isomers **2** and **3**, respectively, indicating reasonable kinetic stability of these structures to isomerization. The computed rotational constants for these isomers should be useful for laboratory and astronomical observation of these species. In addition, four other minimum-energy structures are found to lie somewhat higher in energy. These isomers involve both three- and four-membered carbon rings, as well as a bent-chain structure.

Introduction

The development of radioastronomical techniques over the last three decades has led to the identification of more than 100 molecules in interstellar and circumstellar clouds,[1,2] with species ranging from the familiar (e.g., NH_3) to the exotic (e.g., C_5, a cumulenic dicarbene). Most of the earliest observations were of small molecules (two or three atoms) whose laboratory spectra were well known. More recently, however, molecules containing up to 11 carbon atoms (e.g., the cyanopolyyne $HC_{11}N$)[3] have been detected in sources such as the circumstellar envelope of the carbon-rich star IRC+10216, and even larger chains have been synthesized in the laboratory and proposed for astronomical identification.[4,5]

The series of carbon chain radicals with the general formula C_nH is a particularly unusual class of "nonterrestrial" molecules that has been scrutinized experimentally for values of n up to 14. In 1974, Tucker et al.[6] identified the ethynyl radical C_2H in the Orion nebula, but several years passed before this molecule was detected in laboratory experiments.[7] A similar situation occurred for C_4H which was detected in IRC+10216[8] several years before its laboratory synthesis.[9] In 1986, Cernicharo et al.[10] reported the astronomical identification of the longer chain C_5H and, nearly concurrently, Gottlieb et al.[11] reported its laboratory detection. Since these pioneering studies, technological developments such as Fourier transform microwave spectroscopy have enabled laboratory workers to measure rotational emission spectra of longer and longer carbon chain radicals including the most recent work of Gottlieb et al. on $C_{14}H$.[12]

Theoretical analyses of C_nH radicals have been nearly as comprehensive as their experimental counterparts. The earliest contribution was by Barsuhn[13] whose Hartree−Fock prediction of the rotational constant of linear C_2H was utilized in the work of Tucker et al.[6] described above. The C_3H radical, which is particularly interesting because of its relationship to the abundant interstellar molecule cyclopropenylidene,[14−16] has been studied in both linear[17−21] and cyclic forms.[19,22,23] Longer chains have been examined quantum chemically up to $C_{10}H$,[18,20,24] although

[†] The University of Texas.
[‡] The University of Georgia.

(1) Green, S. *Ann. Rev. Phys. Chem.* **1981**, *32*, 103.
(2) Herbst, E. *Ann. Rev. Phys. Chem.* **1995**, 46, 27.
(3) Bell, M. B.; Feldman, P. A.; Travers, M. J.; McCarthy, M. C.; Gottlieb, C. A.; Thaddeus, *P. Astrophys. J.* **1997**, *483*, L61.
(4) McCarthy, M. C.; Travers, M. J.; Kovács, A.; Gottlieb, C. A.; Thaddeus, P. *Astrophys. J. Suppl. Ser.* **1997**, *113*, 105.
(5) McCarthy, M. C.; Grabow, J. U.; Chen, W.; Gottlieb, C. A.; Thaddeus, P. *Astrophys. J.* **1998**, *494*, L231.
(6) Tucker, K. D.; Kutner, M. L.; Thaddeus, P. *Astrophys. J.* **1974**, *193*, L115.
(7) Sastry, K. V. L. N.; Helminger, P.; Charo, A.; Herbst, E.; Lucia, F. C. D. *Astrophys. J.* **1981**, *251*, L119.
(8) Guélin, M.; Green, S.; Thaddeus, P. *Astrophys. J.* **1978**, *224*, L27.
(9) Gottlieb, C. A.; Gottlieb, E. W.; Thaddeus, P.; Kawamura, H. *Astrophys. J.* **1983**, *275*, 916.
(10) Cernicharo, M.; Kahane, C.; Gómez-González, J.; Guélin, M. *Astron. Astrophys.* **1986**, *164*, L1.
(11) Gottlieb, C. A.; Gottlieb, E. W.; Thaddeus, P. *Astron. Astrophys.* **1986**, *164*, L5.
(12) Gottlieb, C. A.; McCarthy, M. C.; Travers, M. J.; Thaddeus, P. *J. Chem. Phys.* **1998**, *109*, 5433.
(13) Barsuhn, J. *Astrophys. Lett.* **1972**, *12*, 169.
(14) The cyclopropenylidene molecule C_3H_2 has been well-characterized experimentally. For a leading experimental reference, see: Seburg, R. A.; Petterson, E. V.; Stanton, J. F.; McMahon, R. J. *J. Am. Chem. Soc.* **1997**, *119*, 5847.
(15) Vrtilek, J. M.; Gottlieb, C. A.; Thaddeus, P. *Astrophys. J.* **1987**, *314*, 716.
(16) Madden, S. C.; Irvine, W. M.; Matthews, H. E.; Friberg, P.; Swade, D. A. *Astronom. J.* **1989**, *97*, 1403.
(17) Cooper, D. L. *Astrophys. J.* **1983**, *265*, 808.
(18) Cooper, D. L.; Murphy, S. C. *Astrophys. J.* **1988**, *333*, 482.
(19) Jiang, Q.; Rittby, C. M. L.; Graham, W. R. M. *J. Chem. Phys.* **1993**, *99*, 3194.
(20) Woon, D. E. *Chem. Phys. Lett.* **1995**, *244*, 45.
(21) Natterer, J.; Koch, W. *Mol. Phys.* **1995**, *84*, 691.
(22) Yamamoto, S.; Saito, S.; Ohishi, M.; Suzuki, H.; Ishikawa, S.-I.; Kaifu, N.; Murakami, A. *Astrophys. J.* **1987**, *322*, L55.
(23) Stanton, J. F. *Chem. Phys. Lett.* **1995**, *237*, 20.
(24) Pauzat, F.; Ellinger, Y.; McLean, A. D. *Astrophys. J.* **1991**, *369*, L13.

10.1021/ja982532+ CCC: $18.00
Published on Web 02/23/1999

high-accuracy coupled cluster methods have been applied only to those up to C_7H.[20,21]

For C_nH radical carbon chains with $n \geq 4$, all of the experimental and theoretical analyses thus far have dealt with only linear structures. This is due in part to the fact that the linear isomers have relatively simple rotational spectra and are therefore easier to identify in radioastronomical studies. However, the identification of cyclopropenylidene C_3H_2 in several interstellar sources[15,16] more than ten years ago has fueled speculation[25] that a variety of nonlinear molecules could be formed by bimolecular condensation or insertion reactions of C_3H_2 with radical carbon chains or cumulenic bicarbenes via both ion−molecule and neutral−neutral pathways.[26] In fact, quantum chemical studies of C_5H_2 ring-chain isomers have now been reported,[18,27] and the C_5H_2,[28] C_7H_2,[4] and C_9H_2[29] species have recently been synthesized in laboratory Ne-acetylene discharges similar to those used to produce C_nH chains.

In this work, high-level ab initio quantum chemical methods are applied to several isomers of the carbon chain radical C_5H in order to obtain estimates of their rotational constants, relative energetic stabilities, harmonic vibrational frequencies, and dipole moments. These data should assist in the laboratory and astronomical identification of these species and help to elucidate the complex carbon chemistry occurring in the interstellar medium.

Theoretical Methods

The molecular properties of C_5H isomers were computed using coupled cluster methods with two different basis sets. The smaller, denoted DZP, consists of Dunning's contractions[30] ((9*s*5*p*)/[4*s*2*p*] for carbon and (4*s*)/[2*s*] for hydrogen) of Huzinaga's primitive Gaussian basis sets[31] with a set of polarization functions on each atom.[32] The larger basis set, denoted TZ2P, consists of Dunning's contractions[33] ((10*s*6*p*)/[5*s*3*p*] for carbon and (5*s*)/[3*s*] for hydrogen) of Huzinaga's primitive Gaussian basis sets[31] with two sets of polarization functions on each atom.[34] Pure angular momentum functions were used for all d-type orbitals.

Several coupled cluster methods were employed in this work. First, the conventional singles and doubles model,[35] based on a spin-restricted open-shell Hartree−Fock reference determinant (ROHF-CCSD),[36] as well as CCSD augmented with a perturbative estimate of the effects of connected triple excitations [CCSD(T)][37−39] were used. In addition, equation-of-motion coupled cluster (EOM-CC)[40−45] techniques known as EOMIP[46−48] and EOMEA[49,50] were used. In these EOM-based methods, one first solves the CCSD equations corresponding to a nearby closed-shell reference state. For EOMIP this reference corresponds to a related anion, and for EOMEA, a related cation. Using the CCSD wave function parameters, $\hat{T}$, one then diagonalizes the non-Hermitian, similarity-transformed electronic Hamiltonian

$$\bar{H} = e^{-\hat{T}} \hat{H} e^{\hat{T}} \tag{1}$$

in either the space of all h and $2hp$ determinants[51] generated from the $(N + 1)$-electron reference (EOMIP) or the space of all p and $2ph$ determinants[51] generated from the $(N - 1)$-electron reference (EOMEA).[52,53] Finally, a perturbational estimate of the effects of connected triple excitations was included in EOMIP-CCSD energies using the EOMIP-CCSD* approach.[54]

Geometry optimizations were carried out with analytic energy gradients for the CCSD, CCSD(T), EOMIP-CCSD, and EOMEA-CCSD methods described above.[39,55,56] An energy optimum structure was assumed to have been obtained once the root mean square of the internal coordinate forces fell below a threshold of $1.0 \times 10^{-5}\ E_h/a_0$, though some structures were optimized to $1.0 \times 10^{-9}\ E_h/a_0$ due to very flat potential energy surfaces. Harmonic vibrational frequencies and infrared intensities were computed using finite differences of analytic energy gradients and dipole moments computed at geometries displaced from the corresponding stationary point. All computations were carried out with the ACESII package of quantum chemical programs.[57]

Results and Discussion

Using the coupled cluster methods described above, seven minimum-energy structures on the C_5H potential energy surface

(25) Thaddeus, P.; Gottlieb, C. A.; Mollaaghababa, R.; Vrtilek, J. M. *J. Chem. Soc., Faraday Trans.* **1993**, *89*, 2125.
(26) Heath, J. R.; Saykally, R. J. *Science* **1996**, *274*, 1480.
(27) Seburg, R. A.; McMahon, R. J.; Stanton, J. F.; Gauss, J. *J. Am. Chem. Soc.* **1997**, *119*, 10838.
(28) Travers, M. J.; McCarthy, M. C.; Gottlieb, C. A.; Thaddeus, P. *Astrophys. J.* **1997**, *483*, L135.
(29) McCarthy, M. C.; Travers, M. J.; Chen, W.; Gottlieb, C. A.; Thaddeus, P. *Astrophys. J.* **1998**, *498*, L89.
(30) Dunning, T. H. *J. Chem. Phys.* **1970**, *53*, 2823.
(31) Huzinaga, S. *J. Chem. Phys.* **1965**, *42*, 1293.
(32) Redmon, L. T.; Purvis, G. D.; Bartlett, R. J. *J. Am. Chem. Soc.* **1979**, *101*, 2856.
(33) Dunning, T. H. *J. Chem. Phys.* **1971**, *55*, 716.
(34) Gauss, J.; Stanton, J. F.; Bartlett, R. J. *J. Chem. Phys.* **1992**, *97*, 7825.
(35) Purvis, G. D.; Bartlett, R. J. *J. Chem. Phys.* **1982**, *76*, 1910.
(36) Rittby, M.; Bartlett, R. J. *J. Phys. Chem.* **1988**, *92*, 3033.
(37) Raghavachari, K.; Trucks,. G. W.; Pople, J. A.; Head-Gordon, M. *Chem. Phys. Lett.* **1989**, *157*, 479.
(38) Bartlett, R. J.; Watts, J. D.; Kucharski, S. A.; Noga, J. *Chem. Phys. Lett.* **1990**, *165*, 513. Erratum: **167**, 609 (1990).
(39) Gauss, J.; Lauderdale, W. J.; Stanton, J. F.; Watts, J. D.; Bartlett, R. J. *Chem. Phys. Lett.* **1991**, *182*, 207.
(40) Monkhorst, H. J. *Int. J. Quantum Chem. Symp.* **1977**, *11*, 421.
(41) Mukherjee, D.; Mukherjee, P. K. *Chem. Phys.* **1979**, *39*, 325.
(42) Emrich, K. *Nucl. Phys. A* **1981**, *351*, 379.
(43) Ghosh, S.; Mukherjee, D. *Proc. Indian Acad. Sci., Chem. Sci.* **1984**, *93*, 947.
(44) Sekino, H.; Bartlett, R. J. *Int. J. Quantum Chem. Symp.* **1984**, *18*, 255.
(45) Stanton, J. F.; Bartlett, R. J. *J. Chem. Phys.* **1993**, *98*, 7029.
(46) Kaldor, U. *Theor. Chim. Acta* **1991**, *80*, 427.
(47) Mukhopadhyay, D.; Mukhopadhyay, S.; Chaudhuri, R.; Mukherjee, D. *Theor. Chim. Acta* **1991**, *80*, 441.
(48) Rittby, C. M. L.; Bartlett, R. J. *Theor. Chim. Acta* **1991**, *80*, 469.
(49) Nooijen, M. *The coupled cluster Green's function.* Ph.D. Thesis, Vrije Universiteit Amsterdam, 1992.
(50) Nooijen, M.; Bartlett, R. J. *J. Chem. Phys.* **1995**, *102*, 3629.
(51) The notation used here to refer to the EOM diagonalization bases indicates the number of one-electron hole (h) and particle (p) states by which the determinant basis differs from the single-determinant anion (EOMIP) or cation (EOMEA) reference. For example, the set of h determinants is composed of all possible determinants produced by removal of a single electron from the reference, while the set of $2ph$ determinants is produced by removing one electron and adding two electrons to the reference. See refs 52 and 53 for further details.
(52) Bartlett, R. J.; Stanton, J. F. In *Reviews in Computational Chemistry*; Lipkowitz, K. B., Boyd; D. B., Eds.; VCH Publishers: New York, 1994; Vol. 5, Chapter 2, pp 65−169.
(53) Bartlett, R. J. In *Modern Electronic Structure Theory*; Yarkony, D. R., Ed.; *Advanced Series in Physical Chemistry*; World Scientific: Singapore, 1995; Vol. 2, Chapter 16, pp 1047−1131.
(54) Stanton, J. F.; Gauss, J. *Theor. Chim. Acta* **1996**, *93*, 303.
(55) Stanton, J. F.; Gauss, J. *J. Chem. Phys.* **1994**, *101*, 8938.
(56) Crawford, T. D.; Stanton, J. F.; Gauss, J.; Kadagathur, N. S., to be published.
(57) Stanton, J. F.; Gauss, J.; Watts, J. D.; Lauderdale, W. J.; Bartlett, R. J. ACES II. The package also contains modified versions of the MOLECULE Gaussian integral program of J. Almlöf and P. R. Taylor, the ABACUS integral derivative program written by T. U. Helgaker, H. J. Aa. Jensen, P. Jørgensen, and P. R. Taylor, and the PROPS property evaluation integral code of P. R. Taylor.

Table 1. Coupled Cluster Predictions of Structural Data (Bond Lengths (Å), Rotational Constant (MHz)), the Dipole Moment (D),[a] Harmonic Vibrational Frequencies (cm^{-1}), and Infrared Absorption Intensities (km/mol) for the $^2\Pi$ Ground State of Linear C_5H (**1**)

	DZP			TZ2P	
	EOMEA-CCSD	CCSD	CCSD(T)	EOMEA-CCSD	CCSD
$r(C_1-H)$	1.073	1.074	1.075	1.061	1.063
$r(C_1-C_2)$	1.235	1.233	1.245	1.216	1.214
$r(C_2-C_3)$	1.363	1.368	1.358	1.346	1.351
$r(C_3-C_4)$	1.274	1.268	1.285	1.256	1.251
$r(C_4-C_5)$	1.342	1.351	1.345	1.319	1.328
B_e	2317	2312	2302	2385	2380
μ_z	4.421	4.369	4.663	4.553	4.504
$\omega_1(\sigma^+)$	3492.1	3475.0	3450.0	3478.1	3462.4
$\omega_2(\sigma^+)$	2085.2	2105.6	2008.8	2090.6	2111.6
$\omega_3(\sigma^+)$	1941.5	1924.7	1868.2	1944.8	1918.0
$\omega_4(\sigma^+)$	1407.5	1355.0	1375.5	1419.6	1367.5
$\omega_5(\sigma^+)$	741.5	732.3	731.2	747.4	737.7
$\omega_6(\pi)$	695.1	705.4	665.1	715.2	722.8
$\omega_7(\pi)$	521.5	530.3	450.7	526.0	536.2
$\omega_8(\pi)$	512.5	510.6	487.9	534.5	530.7
$\omega_9(\pi)$	326.3	342.5	313.9	357.9	363.2
$\omega_{10}(\pi)$	293.5	310.9	255.6	292.3	337.4
$\omega_{11}(\pi)$	288.4	263.3	254.3	305.0	257.6
$\omega_{12}(\pi)$	172.6	136.3	131.2	167.3	122.1
$\omega_{13}(\pi)$	79.9	103.5	80.9	64.3	109.2
$I_1(\sigma^+)$	95.5	99.4	103.4	91.3	93.4
$I_2(\sigma^+)$	28.8	41.1	19.8	14.4	25.5
$I_3(\sigma^+)$	695.0	458.9	457.6	732.7	515.2
$I_4(\sigma^+)$	98.0	133.8	99.5	89.3	133.7
$I_5(\sigma^+)$	14.5	17.1	10.8	14.2	17.3
$I_6(\pi)$	35.4	32.4	32.2	31.8	29.9
$I_7(\pi)$	52.1	52.5	49.9	52.4	53.1
$I_8(\pi)$	2.7	3.1	1.7	3.8	3.9
$I_9(\pi)$	0.0	0.2	0.1	0.4	0.6
$I_{10}(\pi)$	3.6	3.2	6.9	5.8	4.0
$I_{11}(\pi)$	2.0	5.0	5.4	3.1	7.2
$I_{12}(\pi)$	0.1	1.3	1.8	0.2	1.7
$I_{13}(\pi)$	1.6	0.0	0.0	2.0	0.0

[a] The molecule is oriented as depicted in Figure 1 with the positive *z*-axis to the top of the figure.

have been located and characterized by harmonic vibrational frequency analyses. In addition, several transition states for interconversion among these structures have been identified. In the following subsections, results are presented separately for the three lowest-energy isomers, followed by comparison of their thermal and kinetic stabilities. Data for the remaining isomers are presented in later subsections, followed by energetic comparisons for all isomers as computed at various levels of theory.

Structures and Properties of the Lowest-Energy Isomers. C_5H (1). The highest occupied molecular orbital of the linear isomer of C_5H (hereafter abbreviated *l*-C_5H) is a singly occupied π orbital, giving rise to a $^2\Pi$ electronic state. Hence, the nearest closed-shell configuration is that of $^1\Sigma^+$ C_5H^+, suggesting that EOMEA-CCSD is an appropriate EOM-based method for this isomer. Table 1 summarizes the optimized geometry, rotational constant, dipole moments, harmonic vibrational frequencies, and infrared transition intensities of *l*-C_5H as determined at the EOMEA-CCSD, ROHF-CCSD, and ROHF-CCSD(T) levels of theory using the DZP and TZ2P basis sets described earlier. The highest-level TZ2P/CCSD geometry is depicted in Figure 1.

The geometries given in Table 1 are consistent with the cc-pVTZ/RCCSD(T) results given by Woon;[20] the average difference in computed bond lengths relative to the TZ2P/CCSD level is only 0.01 Å. In addition, the TZ2P/CCSD rotational constant

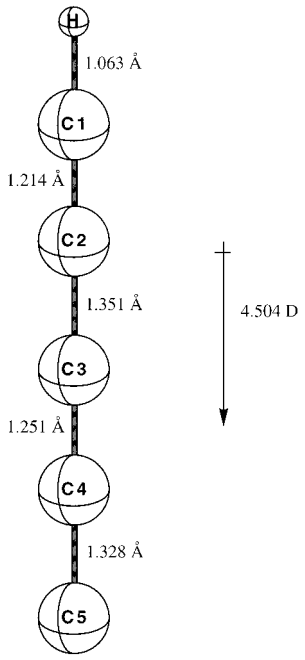

Figure 1. Structure of the $^2\Pi$ ground state of linear C_5H (**1**) determined at the TZ2P/CCSD level of theory. The magnitude and direction of the computed permanent electric dipole are also indicated.

of 2380 MHz given in Table 1 compares nicely with the observed values of 2387 (ref 10) and 2395 MHz (ref 11). It is perhaps reasonable to associate the alternating C−C bond lengths reported in Table 1 with single and triple bonds, although these are somewhat distorted from what is commonly expected.[58] Linear C_5H could therefore be considered to be composed of acetylenic units, with the unpaired electron residing primarily on the terminating carbene carbon atom. Another reasonable Lewis structure, however, is one with a cumulenic bonding pattern and with negative and positive formal charges assigned to the terminal and hydrogen-attached carbons, respectively. Such a structure not only explains the shortened C−C single bonds and elongated triple bonds reported in Table 1, but due to the required charge shift, also explains the large dipole moment (ca. 4.5 D) computed for this isomer. Both of these resonance structures, as well as others with the radical center at carbons 1 and 3, are supported by the DZP/EOMEA-CCSD spin density distribution, and the electronic structure of *l*-C_5H can readily be understood as a weighted average of these representations.

No vibrational spectrum has ever been measured for *l*-C_5H; calculated harmonic vibrational frequencies and associated infrared transition intensities are represented for the first time in this work. There is a relatively close comparison between the EOMEA-CCSD- and ROHF-based coupled cluster frequencies, suggesting that no serious deficiencies are present in the theoretical approach. The most intense transition is the ω_3 C−C stretching mode with a frequency of around 1918.0 cm^{-1}. The Renner−Teller splittings of the π-symmetry linear bending frequencies range from about 20 to 180 cm^{-1}. The shifts in harmonic vibrational frequencies upon single-atom ^{13}C substitution as computed at the TZ2P/EOMIP-CCSD level of theory are given in Table 10. For the linear isomer, the largest shifts are observed in stretching vibrations ω_2 and ω_3 as carbons 2, 3, and 4 are isotopically substituted.

In addition, the optimized geometry of an excited $^2\Sigma^+$ electronic state of *l*-C_5H which is accessible from the nearest

(58) Allen, F. H.; Kennard, O.; Watson, D. G.; Brammer, L.; Orpen, A. G.; Taylor, R. *J. Chem. Soc., Perkin Trans. 2* **1987**, S1.

closed-shell cation has been computed at the DZP/EOMEA-CCSD level of theory. The minimum-energy structure obtained represents a C_3 dicarbene weakly bound to an ethynyl radical C_2H with an intermolecular distance of 2.4 Å. This structure, however, appears to be bound artifactually by basis superposition effects, since inclusion of diffuse *p* functions in the carbon basis [α_p(C) = 0.034] substantially increases the intermolecular distance (to ca. 3.0 Å). Indeed, the total energy of the separated C_3 and C_2H fragments is approximately 5 kcal/mol *lower* in energy than the geometry computed at the DZP/EOMEA-CCSD level of theory. This suggests, then, that this $^2\Sigma^+$ state of the C_5H radical chain is not bound but instead dissociates to C_3 $(\Sigma)_g^{1+}$ and C_2H ($^2\Sigma^+$) fragments lying ca. 110 kcal/mol above the ground $^2\Pi$ electronic state. This observation may serve to explain why there have thus far been no spectroscopic observations of $^2\Sigma \leftarrow {}^2\Pi$ electronic transitions for the $C_{2n+1}H$ radicals while these same transitions for the $C_{2n}H$ series are well known. However, such transitions have been recently observed for the CCN radical,[59] which is isoelectronic to C_3H. A theoretical analysis by Yamashita and Morokuma in 1987[60] on this species determined that the most important electronic configuration for its lowest $^2\Sigma^+$ state is [core]$6\sigma^2 1\pi^4 7\sigma 2\pi^2$, in a low-spin doublet coupling. Analogous configurations may also be important for the C_3H and C_5H radicals, and further theoretical and experimental analyses are necessary before any speculation concerning the thermodynamic stability of this electronic state in these species can be offered.

HC_2C_3 (2). Table 2 reports the computed geometry, rotational constants, components of the electric dipole moment, harmonic vibrational frequencies, and infrared transition intensities for the HC_2C_3 isomer (**2**) of C_5H, and Figure 2 depicts the TZ2P/CCSD geometry. On the basis of its similarities with cyclic C_3H (hereafter abbreviated as *c*-C_3H), the ground electronic state for this structure is expected to be $^2B_2$ with a Hartree−Fock reference configuration of [core]$2b_1^2 10a_1^2 4b_2$. However, based on further comparison to *c*-C_3H as well as Lewis structure arguments, there should also exist a low-lying $^2A_1$ excited state whose Hartree−Fock electronic configuration ([core]$2b_1^2 10a_1 4b_2^2$) must be included in the correlated wave function to obtain a qualitatively correct description of vibrational distortions which lower the symmetry of the nuclear framework (and thereby mix the electronic states). Since both $^2B_1$ and $^2A_1$ electronic configurations are accessible via single-electron removal from the related anion, C_5H^-, EOMIP-CCSD is an appropriate EOM-based method for this isomer.

The C−C bond length of 1.205 Å (TZ2P/CCSD) on the ethynyl chain (see Table 2 and Figure 2) is somewhat shorter than that of the analogous bond in *l*-C_5H and is very close to that of free acetylene, suggesting triple bond character. In addition, the C_3 ring is only slightly distorted relative to *c*-C_3H: in HC_2C_3, the C_{2v}-equivalent C−C bond length of 1.383 Å at the TZ2P/EOMIP-CCSD level of theory is only 0.01 Å longer than that of the same bonds in *c*-C_3H at the same level of theory.[23] In addition, the structure of the HC_2C_3 isomer appears to be closely related to that of ethynylcyclopropenylidene (HC_2C_3H) and could be formed by abstraction or photodissociation of the ring hydrogen in the structure shown (cf. isomer **6** of ref 27). Furthermore, the fairly large dipole moment (see Table 2) for this isomer (ca. 3.4 D at the TZ2P/CCSD level of theory) may be understood using Lewis structure arguments analogous to those used for *l*-C_5H in the previous section.

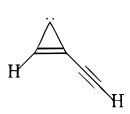

Spin density distributions (computed at the DZP/EOMIP-CCSD level of theory) indicate that the unpaired electron resides primarily on the C_{2v}-equivalent ring carbons, suggesting either an appropriate delocalized Lewis structure or a pair of symmetry-broken resonance structures in which these two carbons alternate between carbene and radical character. This orbital-based interpretation of the electronic structure of isomer **2** is particularly important in elucidating the unusual behavior of the ω_g b_2-symmetry harmonic vibrational frequency (see Table 2), which corresponds to an in-plane "wag" of the C_3 ring. The ROHF-based coupled cluster methods all give a frequency with a magnitude in excess of 1300 cm^{-1}, very high for a bending vibration of this type. These predictions are expected to be qualitatively incorrect, however, due to a near singularity in the ROHF molecular orbital (MO) Hessian at the respective optimized geometries. For example, the MO Hessian at the DZP/CCSD optimized geometry has a very small eigenvalue of only −0.004. This "orbital instability", which results from an

Table 2. Coupled Cluster Predictions of Structural Data (Bond Lengths (Å), Angles (deg), and Rotational Constants (MHz)), Dipole Moments (D),[a] Harmonic Vibrational Frequencies (cm^{-1}), and Infrared Absorption Intensities (km/mol) for the Lowest $^2B_2$ State of the HC_2C_3 Isomer (**2**) of C_5H

	DZP			TZ2P	
	EOMIP-CCSD	CCSD	CCSD(T)	EOMIP-CCSD	CCSD
r(H−C_1)	1.075	1.075	1.076	1.062	1.062
r(C_1−C_2)	1.225	1.226	1.234	1.204	1.205
r(C_2−C_3)	1.411	1.413	1.410	1.395	1.397
r(C_3−C_4)	1.403	1.404	1.413	1.383	1.384
θ(C4−C3−C5)	59.6	59.4	59.4	59.2	59.0
A_e	43402	43544	42998	45096	45262
B_e	3415	3406	3387	3505	3497
C_e	3166	3159	3140	3252	3246
μ_z	3.488	3.348	3.417	3.502	3.386
$\omega_1(a_1)$	3474.2	3472.5	3450.3	3470.2	3467.8
$\omega_2(a_1)$	2169.9	2166.6	2102.9	2190.9	2188.2
$\omega_3(a_1)$	1666.9	1658.2	1613.6	1652.4	1645.8
$\omega_4(a_1)$	1270.7	1283.2	1240.4	1278.7	1292.3
$\omega_5(a_1)$	727.0	724.2	714.6	727.8	725.1
$\omega_6(b_1)$	699.0	688.8	656.0	721.5	713.8
$\omega_7(b_1)$	517.0	515.8	498.0	538.8	538.3
$\omega_8(b_1)$	199.0	201.7	193.1	202.2	205.1
$\omega_9(b_2)$	201.7i	1386.4	1369.4	365.4	1605.2
$\omega_{10}(b_2)$	647.3	634.6	595.5	672.4	662.7
$\omega_{11}(b_2)$	481.6	462.6	440.7	526.5	512.5
$\omega_{12}(b_2)$	246.2	177.9	170.6	131.6	196.1
$I_1(a_1)$	62.5	65.4	65.1	58.1	62.0
$I_2(a_1)$	93.7	74.0	83.7	92.9	70.2
$I_3(a_1)$	35.2	38.5	42.8	38.2	39.4
$I_4(a_1)$	68.2	72.1	63.5	75.3	77.7
$I_5(a_1)$	0.0	0.0	0.0	0.0	0.0
$I_6(b_1)$	34.0	36.5	37.2	31.5	34.0
$I_7(b_1)$	7.4	6.6	4.6	13.7	13.4
$I_8(b_1)$	0.2	0.2	0.2	0.4	0.3
$I_9(b_2)$	568.3	268.8	350.2	566.3	1118.2
$I_{10}(b_2)$	52.9	47.7	48.9	45.7	41.5
$I_{11}(b_2)$	16.4	2.8	0.5	13.7	6.9
$I_{12}(b_2)$	218.9	0.3	0.4	122.3	0.9

[a] The molecule is oriented as depicted in Figure 2 with the positive *z*-axis to the top of the figure.

(59) Kohguchi, H.; Ohshima, Y.; Endo, Y. *J. Chem. Phys.* **1997**, *106*, 5429.

(60) Yamashita, K.; Morokuma, K. *Chem. Phys. Lett.* **1987**, *140*, 345.

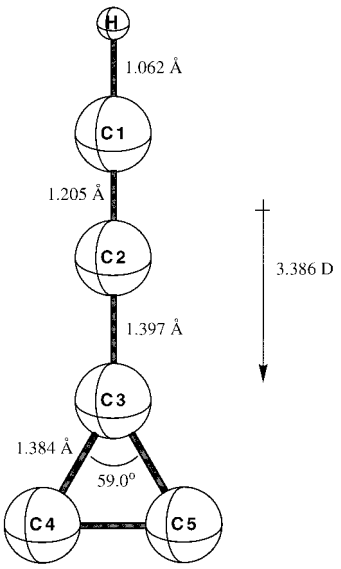

Figure 2. Structure of the lowest $^2B_2$ state of the HC_2C_3 isomer (**2**) of C_5H determined at the TZ2P/CCSD level of theory. The magnitude and direction of the computed permanent electric dipole are also indicated.

energetic competition between the delocalized and symmetry-broken resonance structures described above, may be expected to artifactually affect harmonic vibrational frequencies (or other properties) in the b_2-symmetry block.[61]

The EOMIP-CCSD harmonic vibrational frequencies, on the other hand, do not suffer from such instabilities since they are based on molecular orbitals describing a closed-shell electronic state. They are, however, quite basis set dependent, giving values of 202*i* cm^{-1} (DZP) and 365 cm^{-1} (TZ2P). This behavior most likely results from a second-order Jahn−Teller interaction between the ground $^2B_2$ state and the lowest $\tilde{A}^2$ A_1 state. This interaction is probably overemphasized with the smaller basis set, leading to a negative curvature of the b_2-symmetry potential surface along the ω_9 normal mode. With the larger basis set, the vibronic interaction is apparently smaller, and the given C_{2v}-constrained structure is a minimum on the potential energy surface. This interpretation is supported by the DZP/- and TZ2P/EOMIP-CCSD $\tilde{A}$ $^2A_1 \leftarrow \tilde{X}^2$ B_2 vertical excitation energies of 27.1 and 30.6 kcal/mol, repectively, computed at the $^2B_2$ optimized geometries. By assuming that the transition matrix element connecting the two electronic states through the Q_9 normal coordinate depends only neglibly upon the basis set, a linear relationship between ω_9 and the reciprocal of the vertical excitation energy may be obtained[62] in which the value of ω_9 in the absence of the vibronic interaction with the $\tilde{A}$ state would be *ca.* 1207 cm^{-1}. The EOMIP-CCSD vertical excitation energy as computed with the Dunning cc-pVTZ basis set[63] at the TZ2P/EOMIP-CCSD optimized geometry is 30.5 kcal/mol, leading to an approximate cc-pVTZ/EOMIP-CCSD value for ω_9 of 333 cm^{-1}. Hence, the TZ2P/EOMIP-CCSD value of 365 cm^{-1} appears to be reasonable; it is unlikely that the exact ω_9 frequency exceeds 500 cm^{-1}. Of the remaining well-behaved vibrational modes, several have sufficient relative transition intensities to allow for their identification in infrared analyses. Among the ^{13}C isotopic shifts presented in Table 10, the largest occur for modes 2 and 3 (both a_1-symmetry stretching motions).

C_2C_3H (3). Considering the various ring-chain isomers of C_5H_2 discussed in ref 27, the C_2C_3H isomer (**3**) of C_5H could easily be formed by removal of either the chain hydrogen of ethynylcyclopropenylidene (see the previous section), or one of the ring hydrogens of 3-(didehydrovinylidene)cyclopropene (isomer **8** of ref 27 and simply referred to here as "eiffelene")

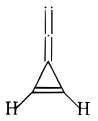

In both cases, this dissociation is expected to produce a $^2A'$ electronic state. Therefore, for consistency with the calculations used for isomer **2** described in the previous section, EOMIP-CCSD as well as ROHF-based coupled cluster methods were used for C_2C_3H. The geometry, rotational constants, dipole moments, harmonic vibrational frequencies, and infrared transition intensities computed for the C_2C_3H isomer (**3**) of C_5H are presented in Table 3. (See also Figure 4.)

Of the two C_5H_2 isomers mentioned above, the geometry of eiffelene bears the stronger resemblance to that of isomer **3**. The C−C bond length of the C_2 chain attached to the ring is stretched by only 0.01 Å in **3** relative to the same bond in eiffelene, and the C_3 ring itself is distorted only slightly. This comparison is also supported by the DZP/EOMIP-CCSD spin density distribution which indicates that the unpaired electron resides most strongly on the ring carbon without the hydrogen. The ethynylcyclopropenylidene isomer of C_5H_2, on the other hand, differs substantially from **3**, with the C−C bond on the carbon chain compressed relative to the latter by more than 0.07 Å as computed at the TZ2P/CCSD level of theory (cf. Table 3 of ref 27). The dipole moment of **3** (5.2 D at the TZ2P/CCSD level of theory) is somewhat diminished relative to that of eiffelene (8.2 D at the same level of theory), but it is still larger than that computed for any of the other isomers examined in this research. In addition, the harmonic vibrational frequencies of C_2C_3H follow the expected trends as the basis set and level of correlation are improved and show no characteristics such as those observed for HC_2C_3 (**2**), lending confidence as to their qualitative accuracy. These facts suggest, then, that a possible route of synthesis for isomer **3** could proceed through photodissociation of the eiffelene isomer of C_5H_2, although further analyses, including examination the dissociation pathway of $C_5H_2 \rightarrow C_5H + H$ are necessary. Furthermore, given the well-established long lifetimes of acetylenic C−H stretching vibrational states,[64] production of isomer **3** through photolysis of the ethynyl chain carbon−hydrogen bond in ethynylcyclopropenylidene should not be ruled out.

Thermal and Kinetic Stabilities. Table 4 summarizes relative energies for the three lowest-energy isomers (structures **1**, **2**, and **3**) of C_5H computed with the TZ2P basis set. Because the EOMIP-CCSD method cannot be appropriately applied to the linear isomer with its singly occupied π orbital (see the discussion above), EOMEA-CCSD single-point energies were

(61) Crawford, T. D.; Stanton, J. F.; Allen, W. D.; Schaefer, H. F. *J. Chem. Phys.* **1997**, *107*, 10626.

(62) This analysis is the same as that used in ref 23 for estimating the magnitude of the Jahn−Teller interaction in *c*-C_3H. Assuming that the ω_9 force constant, *f*, of the $^2B_2$ ground state may be written in terms of the transition matrix element $\langle\psi(^2B_2)|\partial H/\partial Q_9|\psi(^2A_1)\rangle \equiv C^{1/2}$ as

$$f = f_0 - C/\Delta(E)$$

where f_0 is the "non-interacting" force constant and $\Delta(E)$ is the vertical excitation energy between the $^2B_2$ and $^2A_1$ excited states, the DZP/- and TZ2P/EOMIP-CCSD frequencies and excitation energies give a value of $C = 0.002448\ E_h^2/\text{amu-}a_0^2$ and $f_0 = 0.055173\ E_h/\text{amu-}a_0^2$. These values for the slope, *C*, and intercept, f_0, were used to compute the approximate cc-pVTZ/EOMIP-CCSD value of ω_9 discussed in the text.

(63) Dunning, T. H. *J. Chem. Phys.* **1989**, *90*, 1007.

(64) Lehmann, K. K.; Scoles, G.; Pate, B. H. *Ann. Rev. Phys. Chem.* **1994**, *45*, 241.

Table 3. Coupled Cluster Predictions of Structural Data (Bond Lengths (Å), Angles (deg), and Rotational Constants (MHz)), Dipole Moments (Debye),[a] Harmonic Vibrational Frequencies (cm^{-1}), and Infrared Absorption Intensities (km/mol) for the Lowest $^2A'$ State of the C_2C_3H Isomer **(3)** of C_5H

	DZP			TZ2P	
	EOMIP-CCSD	CCSD	CCSD(T)	EOMIP-CCSD	CCSD
$r(C_1-C_2)$	1.296	1.347	1.312	1.275	1.276
$r(C_2-C_3)$	1.339	1.306	1.338	1.320	1.317
$r(C_3-C_4)$	1.464	1.485	1.485	1.444	1.443
$r(C_4-C_5)$	1.360	1.376	1.369	1.336	1.332
$r(C_5-H)$	1.086	1.086	1.088	1.073	1.073
$\theta(C_1-C_2-C_3)$	177.8	178.8	178.0	178.4	178.4
$\theta(C_2-C_3-C_5)$	145.8	147.9	146.3	146.5	146.8
$\theta(C_4-C_3-C_5)$	56.1	56.9	56.0	55.7	55.4
$\theta(C_3-C_5-H)$	140.3	140.4	139.4	140.6	140.5
A_e	35953	35654	35596	37288	37457
B_e	3558	3532	3515	3650	3644
C_e	3238	3214	3199	3325	3321
μ_x	−4.287	−3.264	−3.890	−4.452	−4.716
μ_y	2.183	2.480	2.270	2.150	2.075
$\|\|\mu\|\|$	4.811	4.099	4.504	4.943	5.152
$\omega_1(a')$	3319.4	3311.7	3288.4	3316.3	3316.3
$\omega_2(a')$	2017.4	1961.5	1958.6	2024.2	2012.7
$\omega_3(a')$	1636.5	1613.4	1575.6	1631.5	1632.0
$\omega_4(a')$	1278.7	1110.0	1212.1	1288.1	1226.3
$\omega_5(a')$	991.3	990.6	962.6	999.8	969.3
$\omega_6(a')$	862.9	907.6	790.2	851.0	754.9
$\omega_7(a')$	735.0	702.3	692.9	735.9	732.3
$\omega_8(a')$	420.2	383.7	384.5	448.8	427.7
$\omega_9(a')$	140.6	132.7	122.0	150.5	118.5
$\omega_{10}(a'')$	798.3	804.5	773.7	822.0	814.5
$\omega_{11}(a'')$	501.2	501.1	488.7	510.7	508.8
$\omega_{12}(a'')$	154.1	164.5	150.5	138.9	93.9
$I_1(a')$	29.2	19.0	21.2	33.7	32.0
$I_2(a')$	816.5	304.3	650.5	940.9	755.7
$I_3(a')$	4.1	43.9	9.7	4.9	2.5
$I_4(a')$	1.7	122.0	38.6	4.4	33.0
$I_5(a')$	14.2	67.5	7.6	9.4	5.8
$I_6(a')$	209.0	205.7	272.2	211.7	415.5
$I_7(a')$	13.6	21.7	86.5	17.9	71.3
$I_8(a')$	5.8	1.4	0.9	6.0	1.3
$I_9(a')$	6.1	9.3	6.7	7.1	8.5
$I_{10}(a'')$	37.3	37.0	38.1	35.2	37.1
$I_2(a'')$	0.3	0.3	0.0	0.4	0.6
$I_2(a'')$	2.5	2.4	2.7	3.5	3.9

[a] The components and signs of the dipole moment correspond to the molecule lying in the *xy*-plane as depicted in Figure 4. The positive *x*- and *y*-axes are to the top and right of the figure, respectively.

computed at optimized structures for all three isomers. These geometries were those computed at the TZ2P/EOMEA-CCSD [for *l*-C_5H (**1**)] and TZ2P/EOMIP-CCSD [for HC_2C_3 (**2**) and C_2C_3H (**3**)] levels of theory (see Tables 1, 2, and 3). CCSD and CCSD(T) relative energies were computed at the TZ2P/CCSD optimized geometries reported in Tables 1−3. Due to the errors inherent in the ROHF-based coupled cluster vibrational frequencies for the HC_2C_3 isomer (see the discussion above), all zero-point vibrational energies used to correct the relative energies given in Table 4 were computed using harmonic vibrational frequencies obtained at the appropriate EOM-based coupled cluster method with the TZ2P basis set. The linear isomer **1** is the most thermally stable isomer of C_5H, with the HC_2C_3 isomer (**2**) lying around 5−8 kcal/mol higher in energy. The C_2C_3H isomer (**3**) lies another 17−21 kcal/mol higher than **2**, although it is interesting to note that triple excitations seem to favor **3** and reduce the energy difference relative to isomer **2** to around 17.5 kcal/mol. Otherwise, the ROHF-CCSD, ROHF-CCSD(T), and EOM-based coupled cluster methods are reasonably consistent in these predictions.

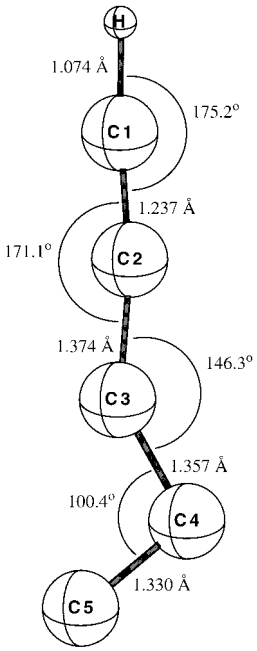

Figure 3. Structure of the $^2A'$ transition state (**2TS**) between the HC_2C_3 isomer (**2**) and the *l*-C_5H isomer (**1**) determined at the DZP/EOMIP-CCSD level of theory.

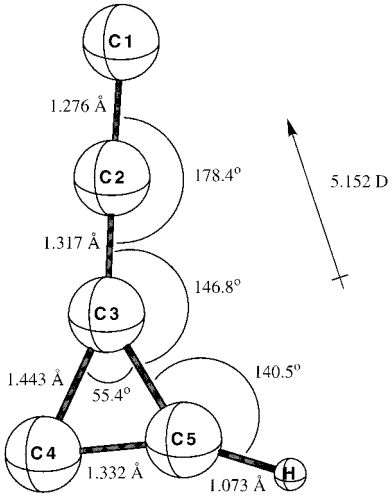

Figure 4. Structure of the lowest $^2A'$ state of the C_2C_3H isomer (**3**) of C_5H determined at the TZ2P/CCSD level of theory. The magnitude and direction of the computed permanent electric dipole are also indicated.

Table 4. Coupled Cluster Predictions of Relative Energies (kcal/mol) for Selected Structural Isomers of C_5H Using a TZ2P Basis Set[a]

isomer	number	electronic state	EOMEA-CCSD	CCSD	CCSD(T)
l-C_5H	**1**	$^2\Pi$	0.0 (0.0)	0.0 (0.0)	0.0 (0.0)
HC_2-C_3	**2**	$^2B_2$	8.2 (8.0)	5.5 (5.3)	6.3 (6.1)
C_2-C_3H	**3**	$^2A'$	27.2 (27.6)	26.4 (26.8)	23.9 (24.1)

[a] Zero-point-corrected values (using the appropriate EOMEA- or EOMIP-CCSD harmonic vibrational frequencies) appear in parentheses. See the discussion given in the text.

Figures 3 and 5 summarize the DZP/EOMIP-CCSD geometries of transition state structures for conversion of isomers **2** and **3**, respectively, into linear C_5H (**1**). The first structure (**2TS**) lies ca. 27 kcal/mol above isomer **2** and is therefore more than

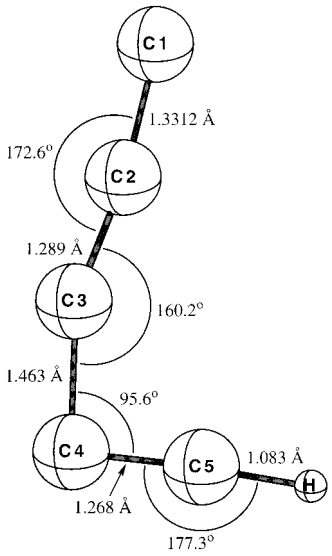

Figure 5. Structure of the $^2A'$ transition state (**3TS**) between the C_2C_3H isomer (**3**) and the *l*-C_5H isomer (**1**) determined at the DZP/EOMIP-CCSD level of theory.

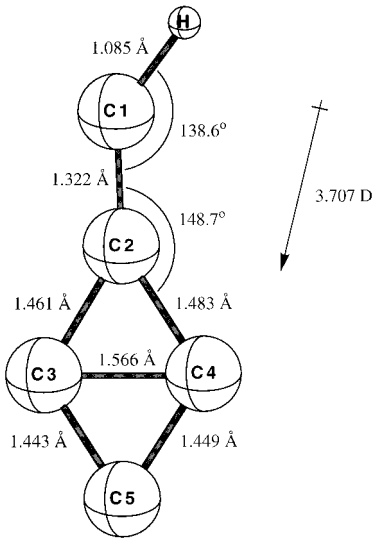

Figure 6. Structure of the lowest $^2A'$ state of the HCC_4 isomer (**4**) of C_5H determined at the DZP/CCSD(T) level of theory. The magnitude and direction of the computed permanent electric dipole are also indicated.

32 kcal/mol above the linear isomer. Its single imaginary harmonic vibrational frequency is 560*i* cm^{-1}. The second transition state **(3TS)** lies around 31 kcal/mol above isomer **3** and is therefore more than 50 kcal/mol above **1**; its imaginary frequency is 694*i* cm^{-1}. Both transition states are formed via simple ring-opening mechanisms from the ring-chain isomers **2** and **3.** Transition state **3TS** is particularly interesting because of its possible similarity to a ring-opening transition state between linear and cyclic C_3H isomers, which have not been investigated theoretically. The significant energy differences among the minimum-energy isomers **1**, **2**, and **3,** as well as between these and the transition states **2TS** and **3TS** indicate reasonable thermal and kinetic stabilities of the three lowest-energy isomers to rearrangement.

Other Isomers. HCC_4 (4). Figure 6 depicts the computed DZP/CCSD(T) geometry of the HCC_4 isomer of C_5H, which involves an unusual four-membered carbon ring. Table 5 summarizes the coupled cluster geometries, rotational constants, and electric dipole moments, as well as DZP/EOMIP-CCSD harmonic vibrational frequencies and infrared transition intensities for this isomer. It is perhaps reasonable to view this structure as a "bridged" attachment of an ethynyl radical (CCH) to a C_3 ring. However, the DZP/EOMIP-CCSD spin density distribution reveals that the unpaired electron resides primarily on the carbon attached to the hydrogen, suggesting instead a CH radical attached to a C_4 ring. This interpretation is supported by comparison of the geometric parameters given in Table 5 and those reported by Watts et al.[65] for rhombic (D_{2h}) C4. At the cc-pVTZ/CCSD(T) level of theory, they obtained a C−C bond length of 1.442 Å, which compares reasonably well to the bond lengths reported in the table, particularly for the carbons at the "bottom" of the ring. The corresponding bond angle [62.6° for $\theta(C_3-C_2-C_4)$ and 65.6° for $\theta(C_3-C_5-C_4)$ at the DZP/CCSD-(T) level of theory] also compares well to the value of 62.75° reported by Watts et al.[65]

Table 5. Coupled Cluster Predictions of Structural Data (Bond Lengths (Å), Angles (deg), and Rotational Constants (MHz)) and Dipole Moments (D),[a] as well as EOMIP-CCSD Harmonic Vibrational Frequencies (cm^{-1}) and Infrared Intensities (km/mol) for the Lowest $^2A'$ State of the HCC_4 Isomer (**4**) of C_5H Using a DZP Basis Set[a]

	EOMIP-CCSD	CCSD	CCSD(T)
$r(H-C_1)$	1.083	1.083	1.085
$r(C_1-C_2)$	1.306	1.316	1.322
$r(C_2-C_3)$	1.453	1.455	1.461
$r(C_2-C_4)$	1.480	1.474	1.483
$r(C_3-C_4)$	1.541	1.545	1.566
$r(C_3-C_5)$	1.430	1.432	1.443
$r(C_4-C_5)$	1.439	1.439	1.449
$\theta(H-C_1-C_2)$	140.8	138.6	138.6
$\theta(C_1-C_2-C_4)$	149.3	149.0	148.7
A_e	34463	34218	33314
B_e	4738	4731	4701
C_e	4165	4156	4120
μ_x	3.501	3.721	3.672
μ_y	0.506	0.502	0.502
$\|\mu\|$	3.537	3.755	3.707
mode	symmetry	frequency	intensity
ω_1	a'	3352.9	37.4
ω_2	a'	1823.4	47.6
ω_3	a'	1465.0	77.4
ω_4	a'	1094.7	5.3
ω_5	a'	977.9	9.0
ω_6	a'	814.5	22.2
ω_7	a'	735.8	55.3
ω_8	a'	524.7	44.3
ω_9	a'	318.2	7.5
ω_{10}	a''	619.5	43.6
ω_{11}	a''	544.0	3.1
ω_{12}	a''	247.7	3.2

[a] The components and signs of the dipole moment correspond to the molecule lying in the *xy*-plane as depicted in Figure 6. The positive *x*- and *y*-axes are to the top and right of the figure, respectively.

The C_s-symmetry structure shown in Figure 6 is only slightly stable with respect to a wagging motion of the hydrogen in the plane; a C_{2v} transition state in which the hydrogen lies along a C_2 axis has been located and shows little distortion of the molecular framework relative to **4** apart from the C−C−H angle. This transition state lies less than 5 kcal/mol above the C_s-symmetry minimum shown in Figure 6.

$CHCC_3$ (5). The $CHCC_3$ isomer (**5**) shown in Figure 7 is somewhat structurally similar to the HC_2C_3 isomer (**2**) in that

(65) Watts, J. D.; Gauss, J.; Stanton, J. F.; Bartlett, R. J. *J. Chem. Phys.* **1992**, *97*, 8372.

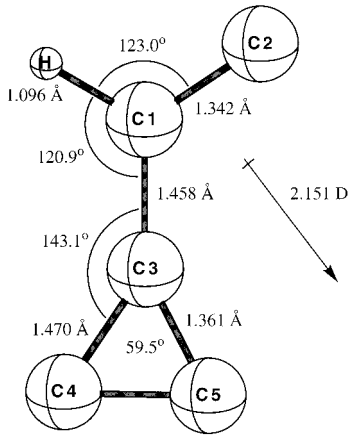

Figure 7. Structure of the lowest $^2A'$ state of the $CHCC_3$ isomer (**5**) of C_5H determined at the DZP/CCSD(T) level of theory. The magnitude and direction of the computed permanent electric dipole are also indicated.

Table 6. Coupled Cluster Predictions of Structural Data (Bond Lengths (Å), angles (deg), and Rotational Constants (MHz)) and Dipole Moments (D),[a] as well as EOMIP-CCSD Harmonic Vibrational Frequencies (cm^{-1}) and Infrared Intensities (km/mol) for the Lowest $^2A'$ State of the $CHCC_3$ Isomer (**5**) of C_5H Using a DZP Basis Set

	EOMIP-CCSD	CCSD	CCSD(T)
$r(H-C_1)$	1.096	1.095	1.096
$r(C_1-C_2)$	1.333	1.336	1.342
$r(C_1-C_3)$	1.456	1.457	1.458
$r(C_3-C_4)$	1.423	1.458	1.470
$r(C_3-C_5)$	1.371	1.352	1.361
$\theta(H-C_1-C_2)$	116.6	119.9	123.0
$\theta(H-C_1-C_3)$	120.3	120.5	120.9
$\theta(C_1-C_3-C_4)$	146.5	143.6	143.1
$\theta(C_4-C_3-C_5)$	60.0	59.7	59.5
A_e	26932	26510	25556
B_e	4063	4101	4157
C_e	3530	3551	3576
μ_x	1.865	1.981	1.884
μ_y	−1.265	−.200	−1.037
$\|\|\mu\|\|$	2.254	1.991	2.151
mode	symmetry	frequency	intensity
ω_1	a'	3190.5	27.3
ω_2	a'	1762.9	153.7
ω_3	a'	1652.1	107.0
ω_4	a'	1291.0	137.9
ω_5	a'	1009.4	15.1
ω_6	a'	809.6	24.7
ω_7	a'	533.0	468.1
ω_8	a'	330.7	92.6
ω_9	a'	154.7	22.2
ω_{10}	a''	654.3	34.3
ω_{11}	a''	402.3	0.7
ω_{12}	a''	98.7	12.2

[a] The components and signs of the dipole moment correspond to the molecule lying in the *xy*-plane as depicted in Figure 7. The positive *x*- and *y*-axes are to the top and right of the figure, respectively.

it can be adequately described as a C_3 ring attached to an ethynyl radical; in this case, however, it is attached to the central carbon of the latter. The geometries summarized in Table 6 support this interpretation in that the C_{2v}-equivalent C−C bond lengths on the ring in **2** are approximately an average of those of the analogous (nonequivalent) C−C bonds in **4**. In addition, according to the DZP/EOMIP-CCSD spin density distribution, the unpaired electron is shared primarily between the terminal ring carbons, suggesting a Lewis structure interpretation of the

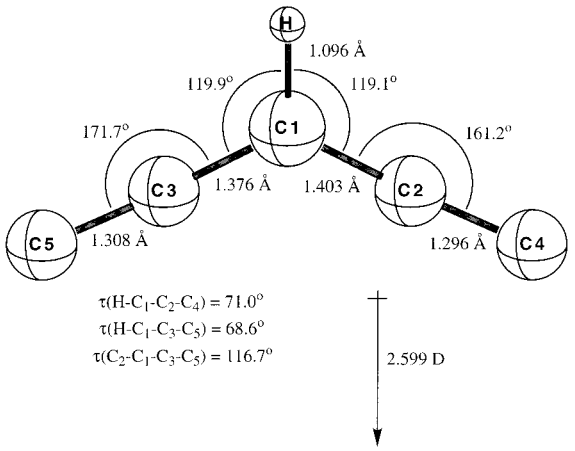

Figure 8. Structure of the lowest ^2A state of the C_2CHC_2 isomer (**6**) of C_5H determined at the DZP/EOMIP-CCSD level of theory. The magnitude and direction of the computed permanent electric dipole are also indicated.

ring similar to that used earlier for isomer **2**. However, the EOMIP-CCSD harmonic vibrational frequencies computed for isomer **4** do not apparently suffer from the same pseudo-Jahn−Teller effects present in isomer **2**, and the values reported in Table 6 are expected to be at least qualitatively correct. It should be noted, however, that isomer **5** may be viewed as a substituted vinylidene, suggesting that a 1,2-hydrogen shift leading to isomer **2** could proceed with only a negligible barrier. Kinetic isolation of isomer **5** seems unlikely.

C_2CHC_2 (6). Other than the linear form (**1**), the symmetrically branched isomer **6** is the only structure examined here that does not involve a three- or four-membered carbon ring. The DZP/EOMIP-CCSD geometry (depicted in Figure 8) is similar to that of ethynylpropadienylidene, which has recently been synthesized and tentatively identified in laboratory experiments,[66] but with the hydrogen removed from the ethynyl chain (see isomer **7** of ref 27). ROHF-based coupled cluster methods such as CCSD and CCSD(T) were not feasible for this isomer due to significant errors in the coupled cluster wave function as indicated by large single excitation ($\hat{T}_1$) amplitudes (ca. 0.7). The DZP/EOMIP-CCSD rotational constants for the C_1 structure shown in Figure 8 are $A_e = 31073$ MHz, $B_e = 2971$ MHz, and $C_e = 2725$ MHz. The geometry is strongly distorted away from C_{2v} symmetry by raising the C_2 chains out of the plane of the figure. The energetic stability of isomer **6** with respect to a C_s transition state in which $r(C_1-C_2)$ and $r(C_1-C_3)$ as well as $r(C_2-C_4)$ and $r(C_3-C_5)$ become equivalent is extremely small, with an energy difference of less than 0.1 kcal/mol at the DZP/EOMIP-CCSD level of theory. DZP/EOMIP-CCSD harmonic vibrational frequencies for this isomer are reported in Table 7, indicating that this isomer is an energy minimum at this level of theory.

CC_3HC (7). The structure of the CC_3HC isomer (**7**) as computed at the DZP/CCSD(T) level of theory is depicted in Figure 9, and the coupled cluster geometries, rotational constants, dipole moments, and DZP/EOMIP-CCSD harmonic vibrational frequencies and intensities are summarized in Table 8. The three central carbon atoms resemble three-membered rings observed in several of the other isomers, although the C−C distance for the C_{2v}-equivalent pair is rather large (1.671 Å). The ground state of the CC_3HC isomer (**7**) of C_5H is of $^2B_1$ symmetry. The DZP/EOMIP-CCSD spin density distribution

(66) Gottlieb, C. A., private communication.

Table 7. EOMIP-CCSD Predictions of Harmonic Vibrational Frequencies (cm^{-1}) and Infrared Intensities (km/mol) for the Lowest ^2A State of the C_2CHC_2 Isomer (**6**) of C_5H Using a DZP Basis Set

mode	frequency	intensity
ω_1	3197.9	0.1
ω_2	1877.2	191.1
ω_3	1465.6	57.3
ω_4	1311.6	41.7
ω_5	992.6	7.6
ω_6	974.0	128.7
ω_7	869.8	15.1
ω_8	406.9	7.6
ω_9	240.6	4.9
ω_{10}	190.5	25.0
ω_{11}	110.1	9.5
ω_{12}	89.9	63.5

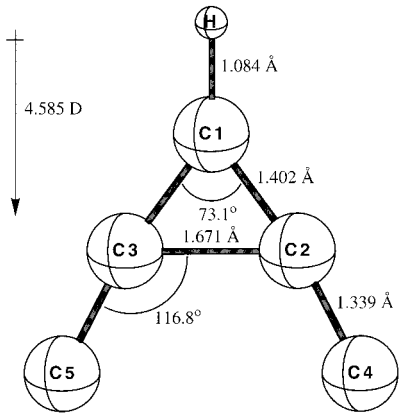

Figure 9. Structure of the lowest $^2B_1$ state of the CC_3HC isomer (**7**) of C_5H determined at the DZP/CCSD(T) level of theory. The magnitude and direction of the computed permanent electric dipole are also indicated.

reveals that the unpaired electron is primarily found on carbon 1, suggesting a simple Lewis structure interpretation of this species in which carbene carbons 4 and 5 are double-bonded to carbons 2 and 3, respectively. Of particular interest is the magnitude of the ω_9 b_2-symmetry harmonic vibrational frequency, which is near 1500 cm^{-1}, somewhat high for an in-plane wagging motion of this type. While these frequency predictions do not suffer from the types of orbital instabilities observed earlier for isomer **2** (the reference determinant is constructed using orbitals from the closed-shell anion), a second-order Jahn−Teller interaction between the $^2B_1$ and a *lower* $^2A_2$ electronic state is possible. However, the $^2A_2$ state lies more than 50 kcal/mol *higher* in energy than the $^2B_1$ state at the DZP/EOMIP-CCSD optimized geometry for the latter state. Further theoretical analyses are required before the ground state of this isomer can be confirmed.

Relative Energetics. Table 9 summarizes the DZP-basis energies of all isomers of C_5H examined here relative to the HC_2C_3 isomer (**2**). The EOMEA-CCSD and EOMIP-CCSD* energies have been computed at the respective EOMIP-CCSD optimized geometries. Energies computed at different levels of theory generally compare to within 4−5 kcal/mol. The effect of connected triple excitations [as estimated using the EOMIP-CCSD* and CCSD(T) methods] varies for the different isomers, although the magnitude of the energy shift is approximately the same for both methods. For example, isomer **5** lies ca. 42.7 kcal/mol higher than isomer **2** at the EOMIP-CCSD level of theory, and EOMIP-CCSD* increases this separation to 44.0 kcal/mol. At the CCSD level, isomer **5** is 42.2 kcal/mol higher than isomer **2**, and the (T) correction increases this to 44.2 kcal/mol, a slightly larger shift than between EOMIP-CCSD and EOMIP-CCSD*.

Table 8. Coupled Cluster Predictions of Structural Data (Bond Lengths (Å), Angles in (deg), and Rotational Constants (MHz)) and Dipole Moments (D),[a] as well as EOMIP-CCSD Harmonic Vibrational Frequencies (cm^{-1}) and Infrared Intensities (km/mol) for the Lowest $^2B_1$ State of the CC_3HC Isomer (**7**) of C_5H Using a DZP Basis Set

	EOMIP-CCSD	CCSD	CCSD(T)
$r(H-C_1)$	1.082	1.082	1.084
$r(C_1-C_2)$	1.399	1.403	1.402
$r(C_2-C_4)$	1.334	1.335	1.339
$\theta(C_2-C_1-C_3)$	69.7	68.8	73.1
$\theta(C_2-C_3-C_5)$	127.4	129.3	116.8
A_e	10904	11106	9779
B_e	6529	6349	7606
C_e	4084	4040	4278
μ_z	4.160	4.117	4.585
mode	symmetry	frequency	intensity
ω_1	a_1	3351.2	41.7
ω_2	a_1	1810.4	7.4
ω_3	a_1	1123.3	5.8
ω_4	a_1	656.5	0.0
ω_5	a_1	94.0	8.2
ω_6	a_2	320.6	0.0
ω_7	b_1	343.9	0.0
ω_8	b_1	139.5	41.1
ω_9	b_2	1498.6	576.8
ω_{10}	b_2	1042.3	20.9
ω_{11}	b_2	826.6	40.0
ω_{12}	b_2	182.6	5.3

[a] The molecule is oriented as depicted in Figure 9 with the positive *z*-axis to the top of the figure.

Table 9. Coupled Cluster Predictions of Energies (kcal/mol) Relative to the HC_2C_3 Isomer (**2**) of C_5H Using a DZP Basis Set[a]

isomer	No.	state	EOMEA-CCSD	EOMIP-CCSD	EOMIP-CCSD*	CCSD	CCSD(T)
l-C_5H	**1**	$^2\Pi$	−6.6	N/A	N/A	−4.1	−4.9
HC_2C_3	**2**	$^2B_2$	0.0	0.0	0.0	0.0	0.0
C_2C_3H	**3**	$^2A'$	16.8	18.2	16.3	18.0	17.1
HCC_4	**4**	$^2A'$	28.3	33.7	37.1	29.4	27.6
$CHCC_3$	**5**	$^2A'$	43.8	42.7	44.0	42.2	44.2
C_2-CH-C_2	**6**	^2A	N/A	49.1	44.8	N/A	N/A
CC_3HC	**7**	$^2B_1$	59.7	64.1	67.6	62.5	62.1

[a] EOMEA-CCSD and EOMIP-CCSD* values have been computed at EOMIP-CCSD optimized geometries for all but the linear isomer, while EOMIP and ROHF-based coupled cluster energies were computed at geometries optimized at the same level of theory.

As Table 9 indicates, isomers **1**, **2**, and **3** lie considerably lower in energy than the other minimum-energy structures, and **2** and **3** are therefore the most likely candidates for new laboratory and/or astronomical identification. Isomer **7** is the highest-energy structure examined in this work, followed by isomers **5** and **6**, which differ in energy by only a few kcal/mol and whose energetic ordering is uncertain. Isomer **4**, which lies about 33 kcal/mol above the linear isomer, might be a candidate for experimental analysis, although no four-membered carbon rings have thus far been observed in either laboratory or interstellar sources.

Summary

The structures and energetics of seven minimum-energy isomers of the carbon-rich radical C_5H have been examined, using high-level coupled cluster methods. Besides the linear structure, which was observed more than a decade ago in radioastronomical experiments, two of the isomers have been

Table 10. Coupled Cluster Predictions of $^{12}C/^{13}C$ Isotopic Shifts (cm^{-1}) in Harmonic Vibrational Frequencies for the Three Lowest-Energy Isomers of C_5H Computed at the EOMIP-CCSD or EOMEA-CCSD Level of Theory Using the TZ2P Basis Set

	normal mode												
carbon	1	2	3	4	5	6	7	8	9	10	11	12	13
						C_5H (**1**)							
1	0	1	2	22	11	5	3	0	2	0	0	1	0
2	0	1	37	11	3	0	0	6	10	3	0	1	0
3	0	1	35	19	0	0	0	11	2	0	3	2	0
4	1	49	1	0	5	0	0	2	0	6	7	0	0
5	12	23	0	6	9	0	0	0	0	2	1	1	0
						HC_2C_3 (**2**)							
1	17	25	2	2	10	0	5	0	1	6	0	1	
2	1	51	0	1	6	2	0	7	1	1	7	3	
3	0	2	29	16	1	3	0	2	3	1	13	1	
4	0	0	15	17	7	3	0	4	1	0	1	0	
						C_2C_3H **(3)**							
1	0	17	7	7	1	0	10	0	3	0	0	2	
2	0	50	2	0	0	0	4	8	2	0	5	3	
3	0	9	15	24	1	12	0	5	1	2	13	1	
4	0	0	19	10	1	8	13	2	1	0	2	1	
5	13	1	19	11	13	6	3	2	1	8	0	0	

found to have reasonable thermodynamic and kinetic stabilities with respect to rearrangement such that they are strong candidates for laboratory and astronomical identification. The remaining isomers, which involve three- and four-membered carbon rings as well as a bent-chain structure, lie somewhat higher in energy, and are therefore less likely to be identified experimentally in the near future.

In addition, we have determined harmonic vibrational frequencies and infrared transition intensities for all seven structures as well as ^{13}C isotopic shifts for the three lowest-lying isomers. Apart from orbital instability problems and an assumed second-order Jahn−Teller interaction for isomer **2**, the harmonic vibrational frequencies are well-behaved, and, in conjunction with the transition intensity and isotopic shift data, should assist in future experimental infrared analyses of these species.

Acknowledgment. This work was supported by the Robert A. Welch Foundation (Texas), the ACS Petroleum Research Fund (Texas), a National Science Foundation Young Investigator Award (J.F.S.), and the Department of Energy (Georgia). The authors wish to thank Dr. Carl Gottlieb (Harvard), Holger Bettinger (Georgia), Professor Lucia Babcock (Georgia), and Professor Nigel Adams (Georgia) for helpful discussions.

JA982532+